Effective parameter (permittivity and permeability) estimator - formulation and user guide

Q-par/AJM/effepsmu/1/v1.3

Q-par Angus Ltd

IDEAS ENGINEERED

Cover + vi + 22 pages

April 2012

Technical Report

Barons Cross Laboratories,
Leominster, Herefordshire, HR6 8RS, UK.
Tel: +44 (0) 1568 612138 Fax: +44 (0) 1568 616373
Web: www.q-par.com E-mail: sales@q-par.com

ADS
Advancing UK Aerospace Defence and Security Industries

Author Q-par Angus Ltd.

Date April 2012

Issued by Q-par Angus Ltd.
Barons Cross Laboratories
Leominster
Herefordshire HR6 HRS
UK.

Document changes record

Issue	Date	Change summary
Issue 1.0	October 2010	First version
Issue 1.1	October 2010	Epsilon-only option
Issue 1.2	October 2010	Further examples
Issue 1.3	April 2012	Included method2 variant for use when S11 data is poor

Abstract

This document provides a brief user and formulation guide for software designed to estimate the effective relative permittivity and permeability from S-parameter measurements of a material slab in free space with a normal incidence plane wave.

List of contents

1 User Guide

1.1 Introduction

This user guide describes the basic algorithm, and the use of software using this algorithm, for estimating the relative complex permittivity ϵ_r and relative complex permeability μ_r of a slab of material in space. It is assumed that the material is homogeneous on a wavelength scale, but not necessarily on a sub-wavelength scale. This allows the method to be employed for meta-materials.

The method is based on a simplification of the method presented in Chen et al. [1] without the use of optimisation methods for materials which are not sufficiently homogeneous. Chen et al. need to consider sets of measurements over materials of varying thicknesses because the materials feature structures (with variations in electrical characteristics normal to the surface of a material) which are insufficiently homogeneous to well define a unique thickness to at material slab. We will assume materials where such inhomogeneity is not a problem.

It is assumed that a slab of unknown material is present in free space with measurements available of the S11 and S21 S-parameters with reference to the ports, port 1 and port 2. It is further assumed that the distances between ports and sample, h_1 and h_2, and the sample thickness d are well defined, given, quantities. It is also assumed that a wave is incident normal to the sample with a defined linear polarisation. Figure 1-1 shows the assumed geometry.

Note that this geometry is well suited to use of the f-solver in CST [2] using periodic boundary conditions with open boundaries in the plus and minus z directions.

If the material is isotropic the direction of the polarisation vector is unimportant and ϵ_r and μ_r are independent of its direction. If the material is anisotropic then this is not generally true. We will assume a material can in general be anisotropic of orthotropic form [3] with the same principal axes that coincide with the x-y-z axes of the measurement configuration. In this case the slab may have a relative permittivity and relative permeability specified by a tensor,

$$\underline{\underline{\epsilon_r}} = \begin{pmatrix} \epsilon_{xx} & 0 & 0 \\ 0 & \epsilon_{yy} & 0 \\ 0 & 0 & \epsilon_{zz} \end{pmatrix} \tag{1-1}$$

and

$$\underline{\underline{\mu_r}} = \begin{pmatrix} \mu_{xx} & 0 & 0 \\ 0 & \mu_{yy} & 0 \\ 0 & 0 & \mu_{zz} \end{pmatrix} \tag{1-2}$$

If the polarisation of the electric field is aligned with the x-direction, then measurement of the s-parameters at normal incidence defines ϵ_{xx} and μ_{yy}. Similarly, if the electric field is aligned with the y-direction, then measurement of the s-parameters at normal incidence defines ϵ_{yy} and μ_{xx}. For any polarisation at normal incidence ϵ_{zz} and μ_{zz} are unmeasurable

and have no effect on the S-parameters. These latter may be determined by a rotation of the sample by 90^o about the x or y-axis.

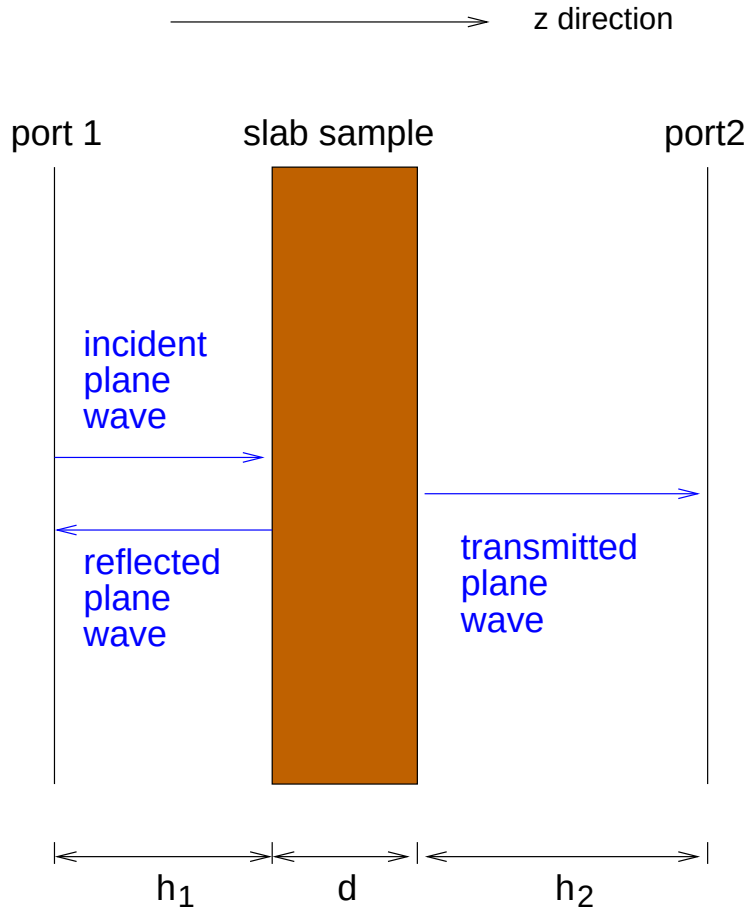

Figure 1-1: Slab excitation by a normal incidence plane wave showing reference ports

1.2 The algorithm

In our formulation we assume a harmonic $\exp(j\omega t)$ time convention associated with an angular frequency ω. Thus all lossy passive materials would be specified by negative imaginary parts to the relative permeability and permittivity. The convention is consistent with the CST f-solver but inconsistent with Chen et al. [1] who employ the alternative $\exp(-i\omega t)$ time convention.[1]

It is assumed that the complex S-parameters are available between ports 1 and 2; S_{11} and S_{21} as a function of frequency. For compatibility with CST, the user specifies four input files containing the amplitude and phase (defined in dB and degrees, respectively) for S_{11} and S_{21} respectively. These would correspond to four CST text export files.

[1] Thus i should be replaced by $-j$ in any field related quantities in [1].

If the amplitudes in dB and phase in degrees are defined by A_{ij} and P_{ij}, associated with the S-parameters then

$$S_{ij}^{(p)} = 10^{0.05\,A_{ij}}\,(\cos(P_{ij}\pi/180) + j\sin(P_{ij}\pi/180)) \tag{1-3}$$

The superfix "p" refers to the fact that these S-parameters are referenced with respect to the ports as illustrated in figure 1-1. We now define the slab S-parameters referenced with respect to the front and rear slab surfaces at each frequency f. These are given by,

$$\begin{aligned} S_{11}(f) &= \exp(+2jk_0h_1)S_{11}^{(p)} \\ S_{21}(f) &= \exp(+jk_0(h_1+h_2))S_{21}^{(p)} \end{aligned} \tag{1-4}$$

where k_0 is the free space wave number, $k_0 = 2\pi f/c_0$, where c_0 is the speed of light in vacuum. It is assumed that h_1 and h_2 are givens.

Following [1], define the refractive index n and the relative characteristic impedance Z (defined relative to the impedance of free space). We then have,

$$\begin{aligned} \mu_r &= nZ \\ \epsilon_r &= n/Z \end{aligned} \tag{1-5}$$

If we define a "characteristic reflection coefficient ", R_{01} by,

$$R_{01} = \frac{Z-1}{Z+1} \tag{1-6}$$

then $S_{11}(f)$ and $S_{21}(f)$ are given by,

$$S_{11} = \frac{R_{01}(1-e^{-j2nk_0d})}{1-R_{01}^2e^{-j2nk_0d}} \tag{1-7}$$

$$S_{21} = \frac{(1-R_{01}^2)e^{-jnk_0d}}{1-R_{01}^2e^{-j2nk_0d}} \tag{1-8}$$

In principal, equations (1-7) and (1-8) are readily inverted to obtain analytic expressions for n and Z such that,

$$Z^2 = \frac{(1+S_{11})^2 - S_{21}^2}{(1-S_{11})^2 - S_{21}^2} \tag{1-9}$$

$$\exp(-jnk_0d) = X \pm j\sqrt{1-X^2} \tag{1-10}$$

where

$$X = \frac{1+S_{21}^2-S_{11}^2}{2S_{21}} \tag{1-11}$$

from which μ_r and ϵ_r may be calculated via (1-5). In practice, there are problems associated with the ambiguity of square roots and obtaining the correct branch cuts in the logarithm required when obtaining n from the exponential. This is where Chen's algorithm becomes

non-trivial. In the presence of noisy data we must allow the possibility of slightly active materials (i.e. ones whose relative permittivity and permeability is specified with a small but positive imaginary part). We must also allow the possibility (sometimes desired) of negative refractive index materials. Also, materials may be electrically thick compared to a wavelength so that the S-parameters, at a single frequency, do not specify the phase delay unambiguously.

First, (1-7) and (1-8) are inverted to obtain,

$$Z = \pm\sqrt{\frac{(1+S_{11})^2 - S_{21}^2}{(1-S_{11})^2 - S_{21}^2}} \tag{1-12}$$

where the sign is chosen in a special manner. First, define a small positive number $\delta_z \ll 1$. (It's not clear what value is best and this is not given in [1]. We currently assume a value $\delta_z = 0.001$ in the algorithm). Physically we require the real part of Z, $\Re(Z)$ to be always positive for a passive material hence we may use this criterion to choose the correct sign in (1-12). However, this is not the best course of action if $|\Re(Z)|$ is very small. Consequently, the sign is chosen according to the following algorithm:

if $|\Re(Z)| \geq \delta_z$ *then choose the sign such that* $\Re(Z) > 0$
else choose the sign such that $|Y| < 1$

where Y is the propagation factor[2],

$$Y = \exp(-jnk_0 d) = \frac{S_{21}}{1 - S_{11}\dfrac{Z-1}{Z+1}} \tag{1-13}$$

There is a further more fundamental difficulty which occurs for frequencies where, in a lossless material, both the numerator and denominator vanish in (1-12). This occurs when $|S_{11}| \to 0$ and $S_{21} \to \pm 1$. In the neighbourhood of frequencies for which this is true, numerical 'noise' will cause ill-conditioning in the determination of Z. At these frequencies there is too little information to unambiguously determine both ϵ_r and μ_r.

The simplest approach is simply not to perform the estimation when this situation occurs and we employ threshold checks using physical measures of performance to decide this. We define three thresholds; one on S11 magnitude in dB, $S11_{dB,thresh}$, one on S21 magnitude in dB, $S21_{dB,thresh}$ and one on S21 phase in degrees, $S21_{deg,thresh}$. If S11 magnitude is sufficiently small and S21 magnitude is sufficiently close to zero dB and the phase of S21 is sufficiently close to a multiple of 180 degrees we say the calculation cannot be performed. To do this, we define the modulo-pi S21 phase, ϕ_π, lying between $-\pi$ and $+\pi$ by the pseudo-code:

[2] for noiseless data both $|Y| \leq 1$ and $\Re(Z) \geq 0$

$\phi_2 = Arg\ (S_{21})\ modulo\ \pi$
if $\phi_2 > \pi/2$ *then* $\phi_\pi = \phi_2 - \pi$
else if $\phi_2 < -\pi/2$ *then* $\phi_\pi = \phi_2 + \pi$
else $\phi_\pi = \phi_2$

and if

(magnitude S_{11} *in dB)* $< S11_{dB,thresh}$
.AND. (magnitude S_{21} *in dB)* $> S21_{deg,thresh}$
.AND. $|\phi_\pi| < S21_{deg,thresh}\ .\pi/180$

then we omit output of ϵ_r and μ_r. By default we assume,

$$\begin{aligned} S11_{dB,thresh} &= -20.0\,\text{dB} \\ S21_{dB,thresh} &= -0.2\,\text{dB} \\ S21_{deg,thresh} &= 10.0\,\text{degrees} \end{aligned} \tag{1-14}$$

More advanced methods (not employed here) require that data is made available from samples of more than one thickness so that full frequency coverage is available. Alternatively, we could interpolate between those frequencies for which good data is available, ideally using a model based scheme using realisable rational functions.

Next we must say something about the frequencies for which we are calculating ϵ_r and μ_r. We assume S-parameter data is available over a span of uniformly sampled frequencies ranging from $f = f_{min}$ to $f = f_{max}$, i.e. we assume sampling at N frequencies, $f = f_i$ such that,

$$f_i = f_{min} + (i-1)f_\delta \text{ for } i = 1, N \tag{1-15}$$

where $f_\delta = (f_{max} - f_{min})/(N-1)$ for $N > 1$. We further assume that f_{min} is such that the material thickness d is small compared to a wavelength in the material. This requires some *a-priori* knowledge of the expected dielectric constant of the material, but is not usually a problem. We also require f_δ such that the difference in phase between contiguous S_{21} (and S_{11}) measurements is small.

Once Z is defined with unambiguous sign, Y is determined using (1-13) whether or not it was used to determine the sign for Z. It is then necessary to unambiguously determine n from Y. In general this cannot be done for a material of arbitrary thickness at a single frequency due to possible phase ambiguity and to avoid the phase ambiguity it is again necessary to use the information available at previous frequencies.

First, define the phase Φ,

$$\Phi = \arctan_2(\Im(Y), \Re(Y)) \tag{1-16}$$

where the $\arctan_2$ function is the quadrant-unambiguous arctangent function, $\Re(Y)$ designates the real part of Y and $\Im(Y)$ designates the imaginary part of Y. Then, the magnitude,

$$R = |Y| \tag{1-17}$$

We then have,

$$nk_0d = j\log_e R - \Phi - 2m\pi \tag{1-18}$$

where m is an (as yet) undefined integer. We have tried two methods to resolve phase ambiguity. The first (used in version v00.00.01 of the software) is probably the simplest and is described as follows:

Method 1

To find m we first note that when $f = f_{min}$, $m = 0$. Also, as the frequency is increased m can jump in value from one frequency to the next by no more than 1. Hence if we define (with subscript notation of any quantity $X_i \equiv X(f_i)$),

$$\Delta_{\phi\, i} = \Phi_i - \Phi_{i-1} \tag{1-19}$$

we may employ the following pseudo-code for each frequency f_i,

$m = 0$
for $i = 2$ *to* N
  if $\Delta_{\phi\, i} < -\pi$ *then* $m \to m + 1$
  else if $\Delta_{\phi\, i} > +\pi$ *then* $m \to m - 1$
end for loop

This defines the value of m to be used in (1-18). Once n is determined from (1-18) and Z is determined from (1-12) then ϵ_r and μ_r are obtained using (1-5).

Method 2 (Chen's method)

Again we assume that $m = 0$ when $f = f_{min}$ and increment the frequency. Here we approximate,

$$\exp\big(-jn(f_i)k_0(f_i)d\big) \approx (1 + \Delta + \Delta^2/2)\exp\big(-jn(f_{i-1})k_0(f_{i-1})d\big) \tag{1-20}$$

where

$$\Delta = -jn(f_i)k_0(f_i)d + jn(f_{i-1})k_0(f_{i-1})d \tag{1-21}$$

The idea is to use this approximation to determine which of the three possibilities for m (m remains unaltered, m increases by 1 or m decreases by 1) on $n(f_i)$ meets most closely the extrapolation (1-20). First, there are two solutions to (1-20) for Δ given by,

$$\Delta = -1 \pm \sqrt{2Y_i/Y_{i-1} - 1} \tag{1-22}$$

with notation $Y_i \equiv Y(f_i)$. Let these solutions be Δ_a and Δ_b. We want $\Im\big(j\Delta + n(f_{i-1})k_0(f_{i-1})d\big)$ to be as close as possible to $\Im\big(n(f_i)k_0(f_i)d\big)$ so define,

$$\begin{aligned} T_a &= |(\Im(j\Delta_a) + \log_e(|Y_{i-1}|) - \log_e(|Y_i|)| \\ T_b &= |(\Im(j\Delta_b) + \log_e(|Y_{i-1}|) - \log_e(|Y_i|)| \end{aligned} \tag{1-23}$$

If $T_a < T_b$ then $\Delta = \Delta_a$ else $\Delta = \Delta_b$.

Our extrapolation then gives an approximation for $\Re\big(n(f_i)k_0(f_i)d\big)$, which we will call $\Re\big(n(f_i)k_0(f_i)d\big)_{est}$, given by,

$$\Re\big(n(f_i)k_0(f_i)d\big)_{est} = \Re(j\Delta) + \Re\big(n(f_{i-1})k_0(f_{i-1})d\big) \tag{1-24}$$

we then test the three integer possibilities, $m(f_i) = m(f_{i-1}) - 1$, $m(f_i) = m(f_{i-1})$ and $m(f_i) = m(f_{i-1}) + 1$ to determine which value of,

$$|(-\Phi_i - 2\pi m(f_i)) - \Re\big(n(f_i)k_0(f_i)d\big)_{est}|$$

is the smallest. That value of $m(f_i)$ which minimises this expression is the one taken for determining $n(f_i)k_0(f_i)d$, i.e.

$$n(f_i)k_0(f_i)d = j\log_e|Y_i| - \Phi_i - 2\pi m(f_i) \tag{1-25}$$

Again, as in method 1, once $n(f_i)$ is determined from (1-25) and Z is determined from (1-12) then ϵ_r and μ_r are obtained using (1-5). Currently Chen's method 2 is implemented though we have not yet found an example where it performs better than method 1.

1.3 Modifications with an assumed $\mu_r = 1.0$, two methods.

1.3.1 Method 1

For many measurement applications it is possible to use the *a-priori* knowledge that the material has an effective relative permeability $\mu_r = 1.0$ (i.e. it is a pure dielectric). In this case the algorithm can be made more accurate because there is more information than is needed for the parameter estimation. In particular, we can avoid the characteristic impedance ambiguity problem at the problematic frequencies where we have employed a threshold.

If the material is fairly lossless, and the measurements remain able to provide accurate phase, the most accurate information is contained in the complex refractive index and we need only calculate the characteristic impedance as a subsidiary quantity to help resolve sign ambiguities.

In algithmic terms, with $\mu_r = 1.0$, we simply compute,

$$\epsilon_r = n^2 \tag{1-26}$$

rather than using (1-5) and ignore the characteristic impedance calculation thresholds in (1-14). We refer to this as *method 1*. This method does, however, still make active use of both the S21 and S11 measurements.

1.3.2 Method 2

There are measurement systems where, due to calibration difficulties[3] the S11 measurements are less reliable than the S21 measurements. In this case it is advantageous to determine ϵ_r, for a given specified μ_r, using only the S21 data. However, such a method requires us to solve (1-8) in isolation and its solution cannot be found in closed form.

We adopt the above *method 1* to provide a first estimate of ϵ_r, $\epsilon_r^{(0)}$, which we use as the start point of a Newton recursion method. We will call this *method 2*. Thus both S11 and S22 are used to provide a stable first estimate $\epsilon_r^{(0)}$ which will nearly always lie sufficiently close to the required solution to ensure rapid convergence. First, from (1-8), we define the fucntion,

$$F(\epsilon_r) = S_{21}(1 - R_{01}^2 e^{-2jk_0dn}) - (1 - R_{01}^2)e^{-jk_0dn} \tag{1-27}$$

where as a function of ϵ_r,

$$R_{01} = \frac{Z(\epsilon_r) - 1}{Z(\epsilon_r) + 1} \tag{1-28}$$

and $n = n(\epsilon_r)$ is the (complex) refractive index. Next we construct its derivative with respect to ϵ_r,

$$F'(\epsilon_r) = -2S_{21}e^{-2jk_0dn}R_{01}\big(R'_{01} - jk_0dR_{01}n'\big) + e^{-jk_0dn}\big((1 - R_{01}^2)jk_0dn' + 2R_{01}R'_{01}\big) \tag{1-29}$$

where the derivatives of n, R_{01} and Z are given by,

$$n' = \frac{n}{2\epsilon_r} \tag{1-30}$$

$$R'_{01} = \frac{2Z'}{(Z+1)^2} \tag{1-31}$$

and

$$Z' = \frac{-Z}{2\epsilon_r} \tag{1-32}$$

In this scheme we require to evaluate the correct branch for the complex square roots in

$$Z(\epsilon_r) = \sqrt{\mu_r/\epsilon_r} \tag{1-33}$$

and

$$n(\epsilon_r) = \sqrt{\epsilon_r\mu_r} \tag{1-34}$$

This is generally non-trivial. My initial belief was that $n(\epsilon_r)$ could be defined such that (as described earlier in the report) $|\exp(-jk_0dn)| \leq 1$ with equality only if both ϵ_r and μ_r are real numbers both positive or (possibly) both negative. However, I found that in the presence of noisy data Newton's method would often fail to converge since this constraint can rapidly shift the expected real part of ϵ_r from positive to negative. If the specified real part of μ_r is restricted to a value greater than zero this is not a problem since in this case we may always take the branch of the square root such that the real part of $n(\epsilon_r)$, $\Re(\epsilon_r) > 0$. In practise this is not an issue since we only wish to use this method when $\mu_r = 1$.

[3] For example in a Gaussian beam system calibration of S11 traditionally requires the use of a precisely positioned perfectly conducting reference plane.

There is less of a problem with determining the correct branch for $Z(\epsilon_r)$ since we require $\Re(Z) \geq 0$ for a passive material, irrespective of values of ϵ_r and μ_r. The only possible problem is when $\Re(Z)$ is nearly zero but this cannot occur for $\mu_r = 1$ (or any number not close to zero).

Newton's method may then be adopted to recursively solve for ϵ_r, using

$$\epsilon_r^{(k+1)} = \epsilon_r^{(k)} - \frac{F(\epsilon_r^{(k)})}{F'(\epsilon_r^{(k)})} \tag{1-35}$$

with initial value for $k = 0$. We limit to a maximum number of iterations, $k \leq k_{max}$ and obtain our estimate $\epsilon_r = \epsilon_r^{(k+1)}$ if the relative error $|F(\epsilon_r)| < \delta_f$ for some very small positive δ_f. Currently we use values for $\delta_f = 10^{-7}$ and $k_{max} = 50$, however in practise we only require about 3 or 4 iterations to obtain convergence in nearly all cases.

2 User guide

Software implementing this algorithm is written in Fortran77 using some common extensions. Current version is standing at v00.00.03 (as of 15 October 2010). It has been compiled using *gfortran* under Linux. If the executable is designated by the command *effeps* then the syntax for execution is,

effeps <*filein*> { *flag1* }

where <filein> is the name of a mandatory input file and *flag1* is an optional flag. *flag1* should either be null (not present), the 3-character string "eps" or a 4-character string "eps0", "eps1" or "eps2". If,

flag1 = '' or flag1 = 'eps0'	S11 and S12 data fully used to determine complex μ_r and complex ϵ_r
flag1 = 'eps' or flag1 = 'eps1'	S11 and S21 data used, but make assumption that $\mu_r = 1.0$ to determine complex ϵ_r (method 1)
flag1 = 'eps2'	S11 used as initial estimate but only S21 is used to obtain final results. Make the assumption that $\mu_r = 1.0$ to determine complex ϵ_r (method 2).

The input file takes the form,

```
<filein1>
<filein2>
<filein3>
<filein4>
d
h1
h2
<fileout>
```

where *filein1* is the file name of the data file containing the S11 magnitudes in dB. *filein2* is the file name of the data file containing the S11 phases in degrees. *filein3* is the file name of the data file containing the S21 magnitudes in dB. *filein4* is the file name of the data file containing the S21 phases in degrees.

d represents the material thickness expressed in mm. $h1$ and $h2$ specify h_1 and h_2 expressed in mm. The input S-parameter files assume formats as used in exported CST text files. These contain two header lines (which are ignored) followed by two columns of data where the first column represents frequency in GHz and the second column the S-parameter magnitude (in dB) or phase (in degrees) as appropriate to the file type.

The frequencies must be sequential and in increasing order. Moreover it is assumed that the same frequency list is used for each of the four files. If the (first) line contains a zero frequency record it is ignored since the algorithm cannot employ a zero frequency.

Outputs specifying the complex ϵ_r and μ_r at the frequency f_i are sent to the file *fileout* provided the data is considered good, as defined by the threshold criteria on the s-parameters discussed previously. The phase jump integer $m(f_i)$ is also output, intended for diagnostic purposes only. If the output is considered bad, and any warning or error messages are sent to standard terminal output for diagnostics.

3 Examples

3.1 Example 1

In this example we employ the frequency domain solver in CST with periodic boundary conditions to obtain the S-parameters from a dielectric slab of uniform dielectric constant $\epsilon_r = 3.5$. We estimate both ϵ_r and μ_r with no *a-priori* assumption on μ_r. The material is chosen to be electrically thick with $d = 50\,mm$ for frequencies between zero and 10 GHz. The distances between ports and sample $h_1 = h_2 = 15\,mm$. Figure 3-1 shows the geometry as employed in CST version 10 with default sampling. Figure 3-2 shows the predicted magnitudes for S_{11} and S_{21} (phases not shown). Figure 3-3 shows the predicted values of the real and imaginary parts of ϵ_r and μ_r.

The predictions are very accurate over the range of defined data. If we had reduced the S-parameter thresholds we would note "glitches" at those frequencies where estimation is not made. There are no problems associated with the change in the value of m (which varies between 0 and -2 over this frequency range).

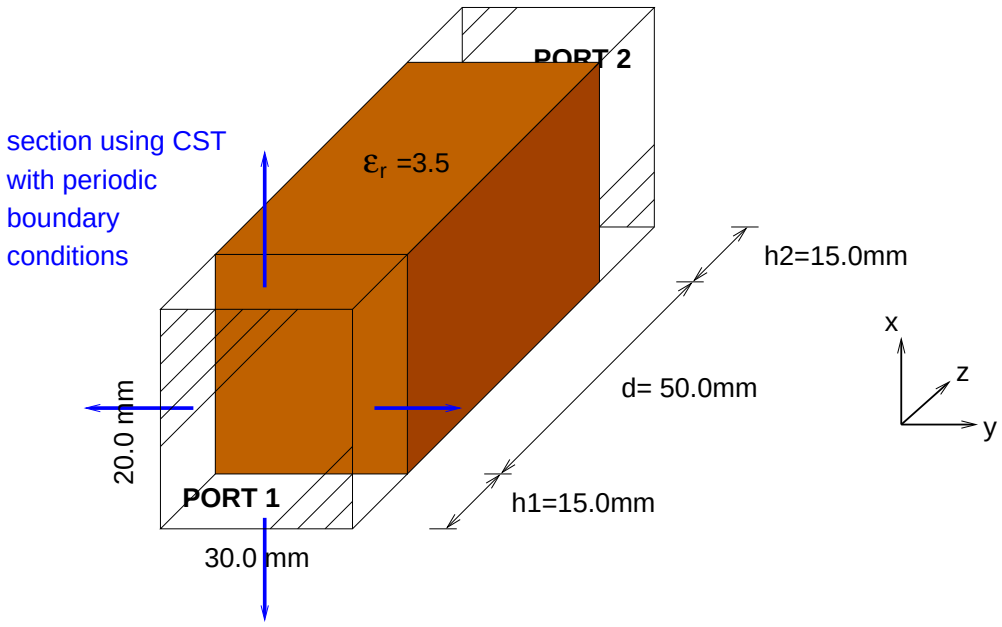

Figure 3-1: Uniform dielectric slab modelled with CST

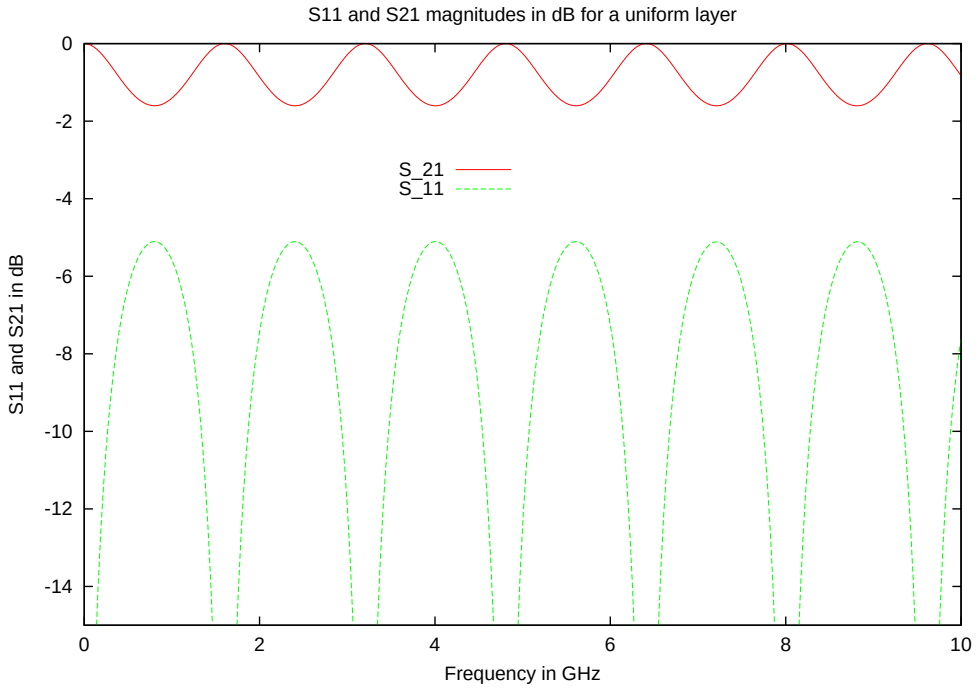

Figure 3-2: Predicted S-parameter magnitudes in dB

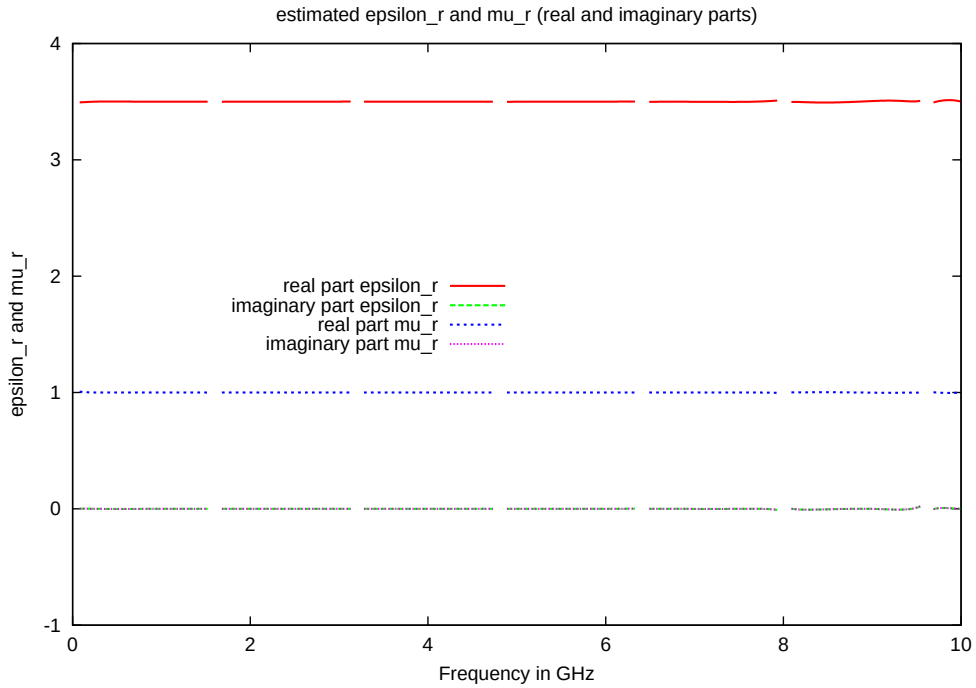

Figure 3-3: Predicted relative permittivity and permeability from S-parameters

3.2 Example 2

In this example we consider a simple metamaterial composed of uniform layers of different dielectrics. The structure is illustrated in figure 3-4. The layers alternate between $\epsilon_r = 3.5$ and $\epsilon_r = 1.5$. Dimensions and CST implementation are as given in example 1.

In this case the effective permittivity is tensorial and dependent on the polarisation of the incident wave. As described in the introduction, the principal axes of the structure are aligned with respect to the x and y axes. So, with the E-field parallel to the x-axis, ϵ_r defines ϵ_{xx} and μ_r defines μ_{yy}. Similarly, with the E-field parallel to the y-axis, ϵ_r defines ϵ_{yy} and μ_r defines μ_{xx}. These results are plotted in figures 3-5 and 3-6.

We first estimate both ϵ_r and μ_r with no *a-priori* assumption on μ_r. The results for ϵ_{xx} and μ_{yy} appear to be less accurate judging by the slight periodic variation between the "bad data" points. This is most likely a consequence of CST since high accuracy requires a fine sampling transverse to the multiple layers. The predictions indicate $\epsilon_{xx} \approx 2.1 \pm 0.02$ and $\epsilon_{yy} \approx 2.5 \pm 0.02$ with remarkably little variation over the frequency range zero to 10 GHz.

Note that because, in this example, the material is actually uniaxial with axis in the x-direction we know that $\epsilon_{zz} = \epsilon_{yy}$ and $\mu_{zz} = \mu_{yy}$. Furthermore, we expect $\mu_{xx} = \mu_{yy} = \mu_{zz} = 1.0$ because there is no z-dependence to the structure and the material components are themselves of unit relative permeability.

We now compare using the command line option *eps* for *flag1*, which makes the *a-priori* assumption that $\mu_r = 1.0$. Predictions are given in figures 3-7 and 3-8. Here there is no evidence of inaccuracy in the neighbourhood of the troublesome frequencies. For example in figure 3-8 the real part of ϵ_r varies fairly uniformly between 2.102 near zero frequency to 2.105 near 10GHz.

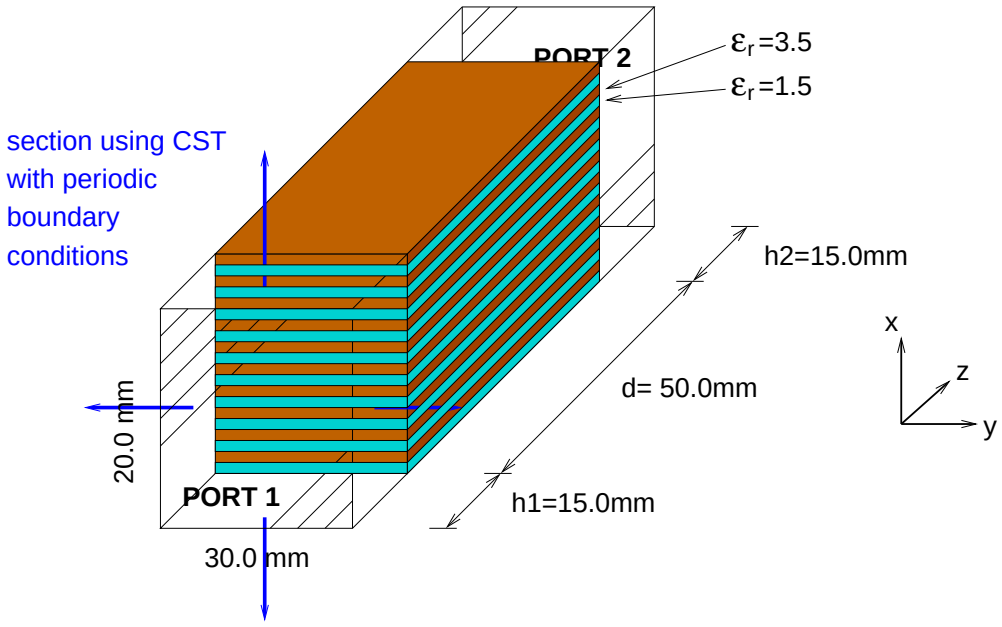

Figure 3-4: layered dielectric slab modelled with CST

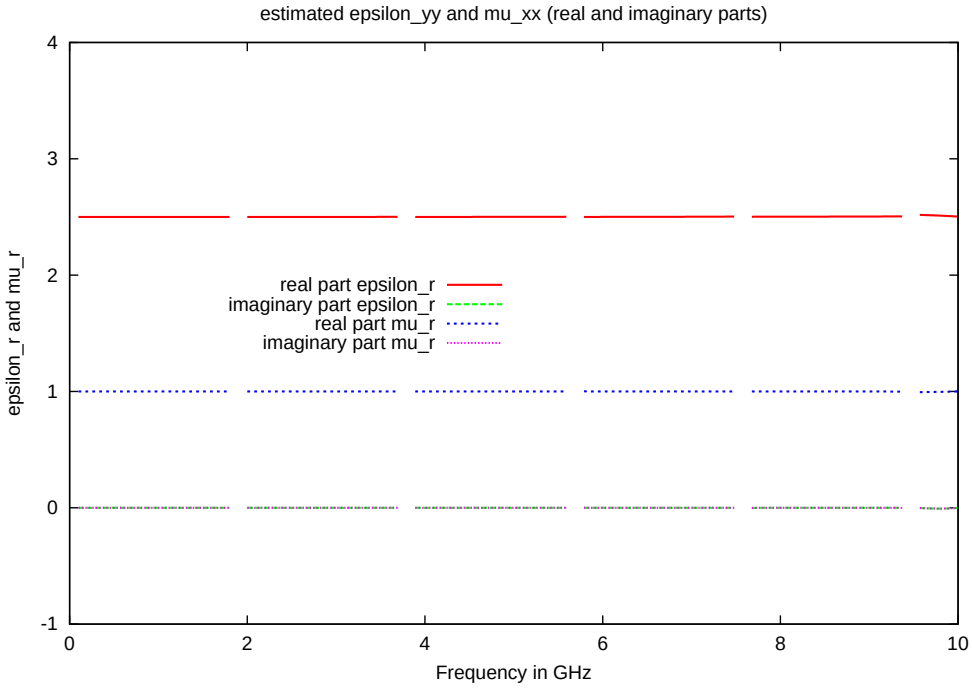

Figure 3-5: Predicted equivalent ϵ_{yy} and μ_{xx} from S-parameters

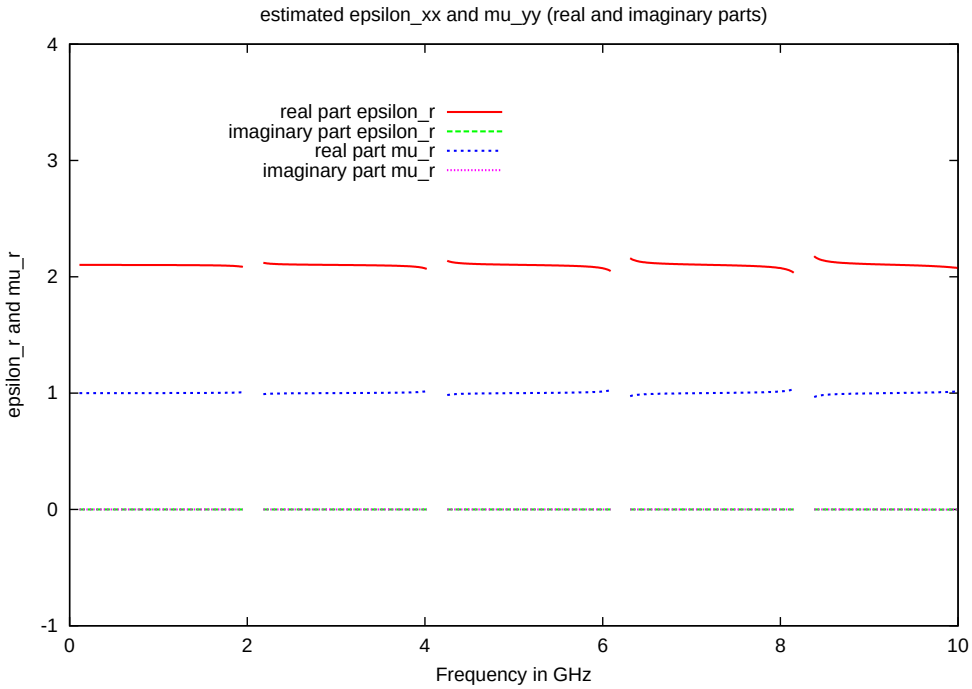

Figure 3-6: Predicted equivalent ϵ_{xx} and μ_{yy} from S-parameters

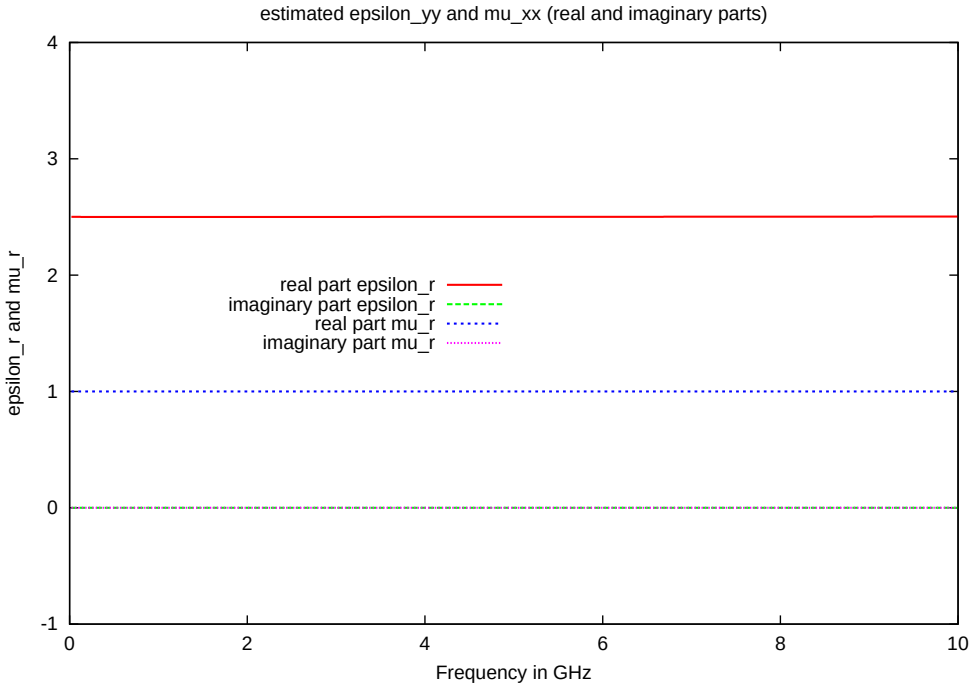

Figure 3-7: Predicted equivalent ϵ_{yy} from S-parameters assuming $\mu_{xx} = 1.0$

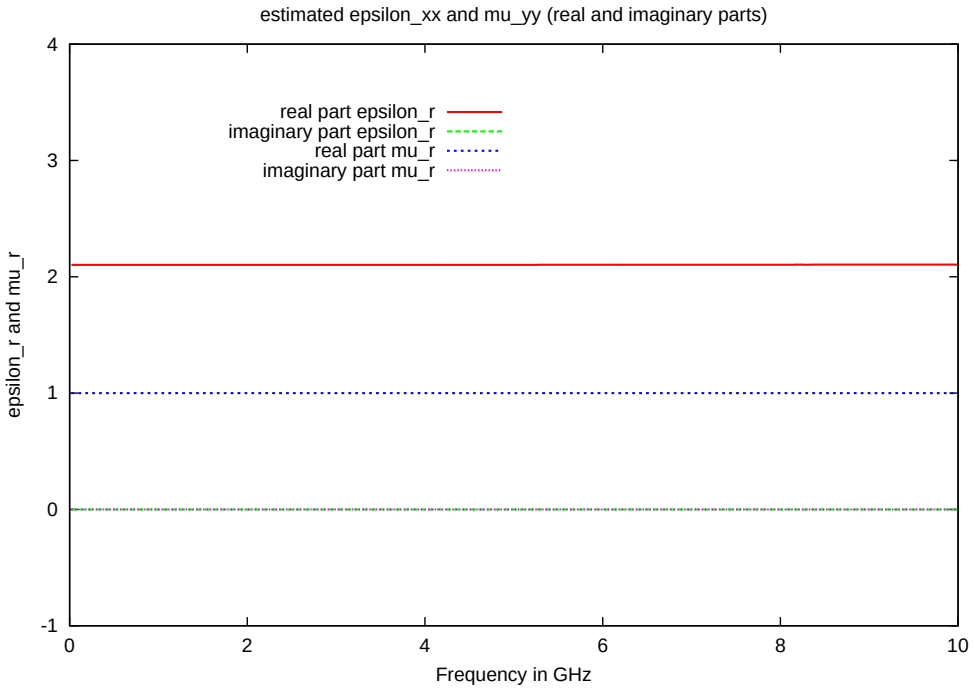

Figure 3-8: Predicted equivalent ϵ_{xx} from S-parameters assuming $\mu_{yy} = 1.0$

3.3 Example 3

In this example we present an orthotropic structure with principal values of permittivity which fall in the correct range for use as part of a composite for a wide-band, angle-insensitive linear to circular polariser. The structure is composed of narrow thin strips of a high dielectric constant, with $\epsilon_r = 6.15$, available as the Rogers material RO6006, in a low dielectric constant substrate comprising layers and strips with $\epsilon_r = 1.2$. This could be implemented using a low density foam material.

Figure 3-9 shows a block of the material and figure 3-10 shows the strip dimensions. The CST f-solver simulations are made using the periodic boundary condition formulation with normal incidence waves in the configuration illustrated and with the block rotated by 90 degrees about the y-axis. This permits us to determine all three principal values of the relative permittivity. Since the structure has an effective relative permeability known to be unity (reasons as given above), we use the "eps" option in our software using this *a-priori* knowledge. Figures 3-11 and 3-12 show the transverse relative permittivities in the un-rotated configuration and 3-13 and 3-14 in the rotated configuration. This shows that between zero to 10 GHz the principal values are almost constant with $\epsilon_{xx} \approx 1.47$, $\epsilon_{yy} \approx 2.14$ and $\epsilon_{zz} \approx 1.80$.

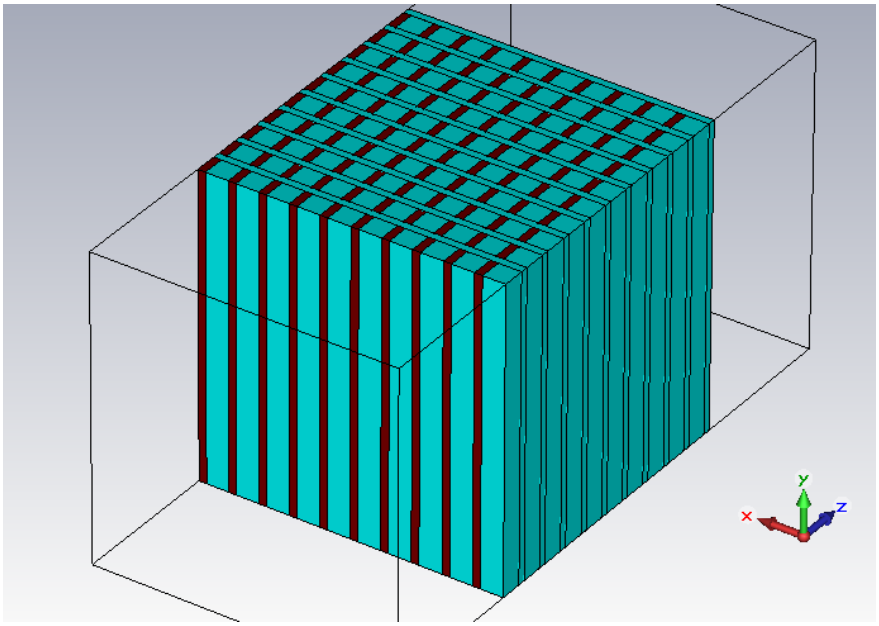

Figure 3-9: CST geometry model comprising high dielectric strips in a low dielectric composite

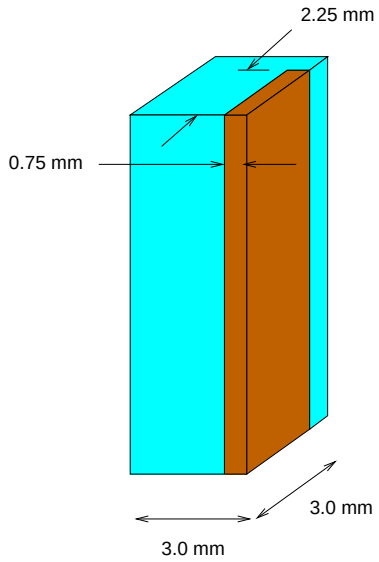

Figure 3-10: Strip dimensions

3.4 A few tentative remarks in the design of orthotropic materials

We have found, using optimisation software in conjunction with anisotropic layer analysis, that the design of wideband linear to circular polarisers generally requires orthotropic materials with relatively small principal values for the relative permittivity tensor, but with moderately large differences between principal values. For example using multiple layers with $(\epsilon_{xx}, \epsilon_{yy}, \epsilon_{zz}) = (2.2, 1.5, 2.3)$, $(2.0, 1.3, 1.6)$ and $(1.5, 1.5, 1.3)$. These materials are then rotated about the z-axis to achieve the necessary polarisation transformations.

To achieve a significant difference in the principal values (e.g. between 1.5 and 2.3) requires a rather larger contrast in the constituent materials; hence the use of a component material with $\epsilon_r = 6.15$. This also requires the percentage volume of the high dielectric to be significantly smaller than that of the low dielectric. Increasing the percentage volume of the high dielectric constant increases the principal values of the effective permittivity but reduces the difference (as a fraction of the average value) between them.

Other methods of achieving orthotropic materials with the right range of principal values have not been properly investigated but it is believed the above rules are still valid. Thus, for example, the use of air filled voids or drill holes in a high dielectric constant is not recomended if a moderately large difference in the principal values is required.

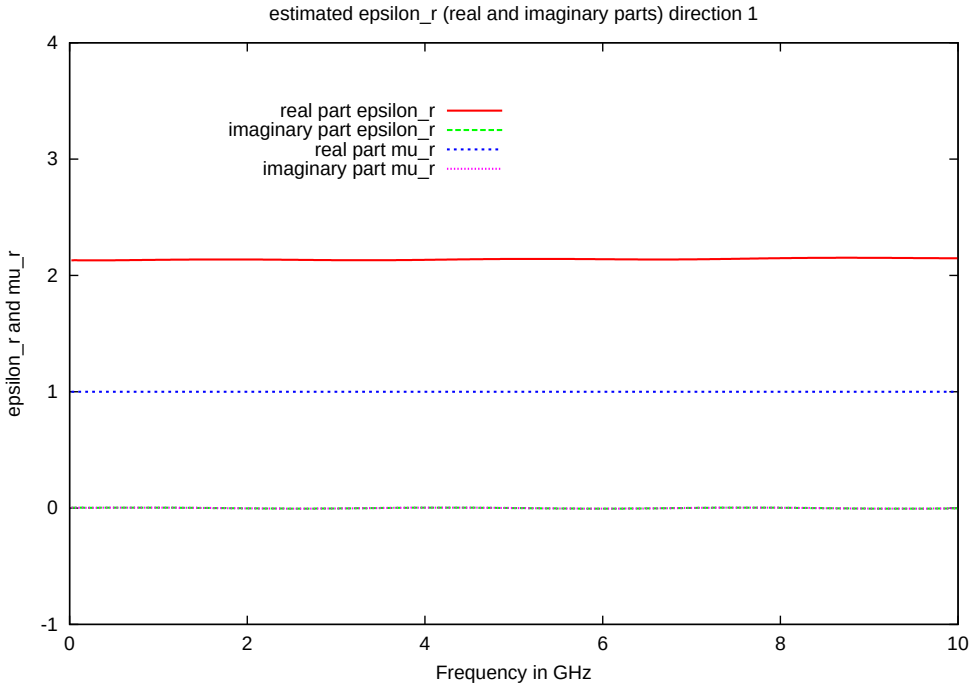

Figure 3-11: Predicted equivalent ϵ_{yy} from S-parameters assuming $\mu_{xx} = 1.0$ from unrotated sample

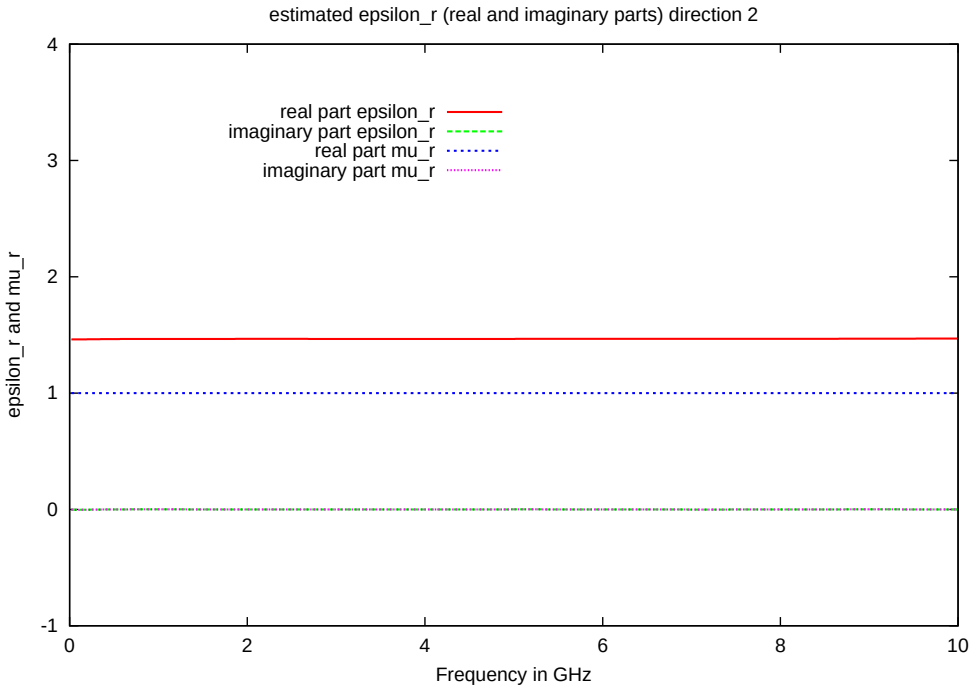

Figure 3-12: Predicted equivalent ϵ_{xx} from S-parameters assuming $\mu_{yy} = 1.0$ from unrotated sample

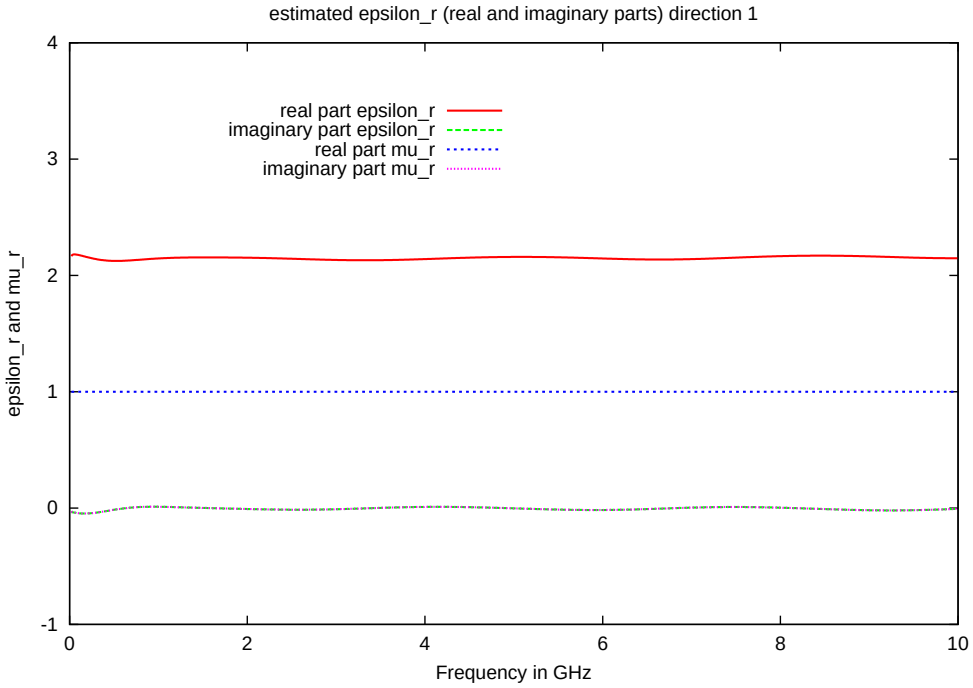

Figure 3-13: Predicted equivalent ϵ_{yy} from S-parameters assuming $\mu_{zz} = 1.0$ from rotated sample

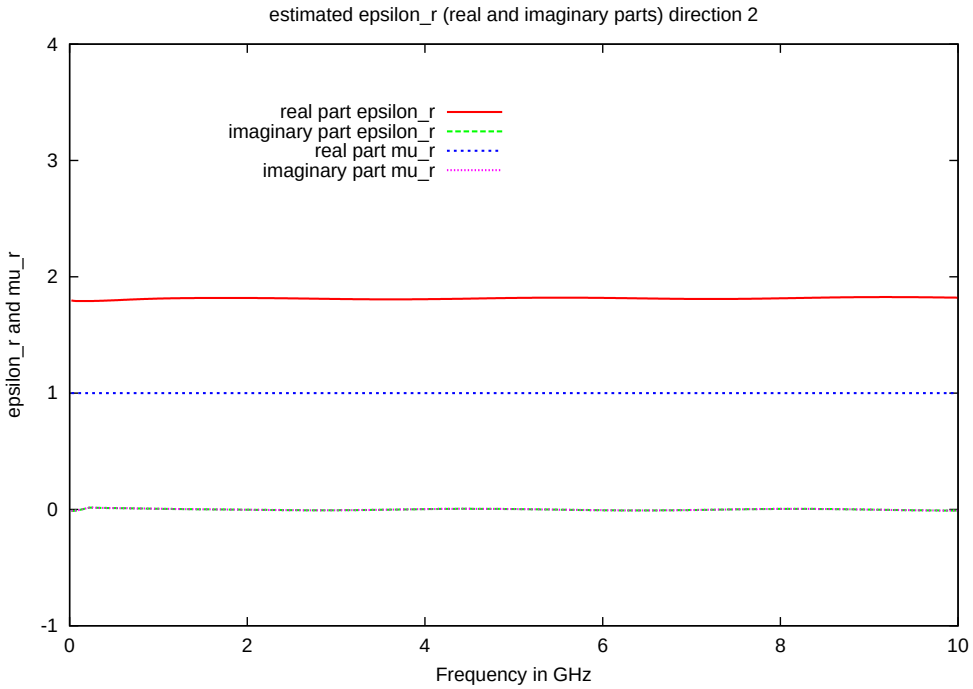

Figure 3-14: Predicted equivalent ϵ_{zz} from S-parameters assuming $\mu_{yy} = 1.0$ from rotated sample

4 References

1 *X. Chen, T.M. Grzegorczyk, B-I Wu, J. Pacheco, J.A. Kong "Robust method to retrieve the constitutive effective parameters of metamaterials"* Physical Review E 70, 016608 (2004), pp1-70.

2 *CST computer simulation technology* See web site: http://www.cst.com/Content/Products/MWS/FrequencyDomainSolver.aspx

3 *Andrew Mackay "Bianisotropic multi-layer analysis software - formulation and user guide* Q-par Angus report: Q-par/AJM/anlay/1/v1.0, September 2010.